A&A 442, 925–928 (2005)
DOI: 10.1051/0004-6361:20053681

Astronomy & Astrophysics

The recurrent ultra-luminous X-ray transient NGC 253 ULX1⋆

M. Bauer and W. Pietsch

Max-Planck-Institut für extraterrestrische Physik, Giessenbachstraße, 85741 Garching, Germany
e-mail: mbauer@mpe.mpg.de

Received 22 June 2005 / Accepted 28 June 2005

ABSTRACT

We present the results of *ROSAT* and XMM-Newton observations of the recurrent ultraluminous X-ray source (ULX) NGC 253 ULX1. This transient is one of the few ULXs that was detected during several outbursts. The luminosity reached 1.4×10^{39} erg s^{-1} and 0.5×10^{39} erg s^{-1} in the detections by *ROSAT* and XMM-Newton, respectively, indicating a black hole X-ray binary (BHXRB) with a mass of the compact object of $\geq$11 $M_{\odot}$. In the *ROSAT* detection NGC 253 ULX1 showed significant variability, whereas the luminosity was constant in the detection from XMM-Newton. The XMM-Newton EPIC spectra are well-fit by a bremsstrahlung model (kT = 2.24 keV, $N_{\rm H} = 1.74 \times 10^{20}$ cm^{-2}), which can be used to describe a comptonized plasma. No counterpart was detected in the optical I, R, B, NUV and FUV bands to limits of 22.9, 24.2, 24.3, 22 and 23 mag, respectively, pointing at a XRB with a low mass companion.

Key words. X-rays: stars

1. Introduction

Ultra-luminous X-ray sources (ULXs) are extra-nuclear compact X-ray sources with luminosities considerably exceeding the Eddington luminosity for stellar mass X-ray binaries of $\sim 2 \times 10^{38}$ erg s^{-1} (Makishima et al. 2000). However their luminosities are still lower than that of active galactic nuclei (AGN).

There are currently four preferred models to explain the luminosities of these objects. The first is that ULXs are intermediate mass black holes (IMBHs: $M_{\rm BH} \sim 10^2$–10^5 $M_{\odot}$). However IMBHs are at present not explainable with stellar evolutionary models. The alternatives are stellar-mass black hole X-ray binaries where either photon bubble instabilities allow super-Eddington luminosities (Begelman 2002), anisotropically emitting X-ray binaries (King et al. 2001), or that ULXs are micro-quasars that are observed down the beam of their relativistic jet (e.g. Reynolds et al. 1997). It is therefore important to increase the sample of ULXs to find arguments that favour or exclude the above models. One attempt was the search for ULXs in 313 nearby galaxies from *ROSAT* HRI observations by Liu & Bregman (2005, hereafter LB2005). A target of this search was the starburst galaxy NGC 253 where they found 21 X-ray sources but only one of them matched their criteria for an ULX (NGC 253 ULX1). This source is located within, but close to the north-east boundary of the D25 ellipse of NGC 253.

We here report on a more detailed analysis of NGC 253 ULX1 including *ROSAT*, XMM-Newton and *Chandra* data, and specifically on the detection of a second outburst in one of the XMM-Newton observations.

⋆ Based on observations obtained with XMM-Newton, an ESA science mission with instruments and contributions directly funded by ESA Member States and NASA.

2. Search for the source in XMM-Newton, Chandra and ROSAT archives

We searched the *ROSAT*, *Chandra* and XMM-Newton archive for observations of NGC 253. The results are listed in Table 1. Except for two *Chandra* observations the position of NGC 253 ULX1 was always in the field of view (FOV). Besides the first detection in *ROSAT* observation 601111h (LB2005), NGC 253 ULX1 was only visible in XMM-Newton observation 0110900101. These XMM-Newton and *ROSAT* HRI data are further discussed in Sects. 3 and 4, respectively.

For the remaining observations we determined 3σ upper limits for the count rate. From that we obtained upper limit for fluxes and luminosities (cf. Table 1). We used WebPIMMS (v3.6c) with the spectral model we got from the analysis of XMM-Newton observation 0110900101 to determine energy conversion factors. The long term light curve of NGC 253 ULX1 is shown in Fig. 2.

3. Detailed analysis of XMM-Newton observation 0110900101

NGC 253 ULX1 was detected for the second time on 2000 December 14 with XMM-Newton. The position of the source was within the FOV of both of the MOS and the PN cameras. We used the latest version of the Science Analysis System (SAS v6.1) to process the obtained data from the PN (thin filter) and the two MOS (medium filter) detectors. Periods of high background were determined and excluded from further analysis. The low background exposure times for PN and for the MOS instruments were 23.0 ks and 24.4 ks, respectively.

Table 1. Individual observations of NGC 253 ULX1.

Date	Instrument	Observation ID	Duration (ks)	Flux[a] (erg cm^{-2} s^{-1})	L_X[a] (10^{39} erg s^{-1})
1991-12-08	*ROSAT*	600088h-0	3.1	$<1.1 \times 10^{-13}$	<0.08
1991-12-25	*ROSAT*	600087p-0	11.6	$<2.2 \times 10^{-14}$	<0.02
1992-06-03	*ROSAT*	600087p-1	11.2	$<4.4 \times 10^{-14}$	<0.03
1992-06-05	*ROSAT*	600088h-1	25.7	$<4.4 \times 10^{-14}$	<0.03
1995-01-03	*ROSAT*	600714h	11.0	$<5.2 \times 10^{-14}$	<0.04
1995-06-13	*ROSAT*	600714h-1	19.8	$<2.0 \times 10^{-14}$	<0.02
1997-12-20	*ROSAT*	601111h	17.5	1.8×10^{-12}	1.4
1998-07-01	*ROSAT*	601113h	2.0	$<2.8 \times 10^{-13}$	<0.2
1999-12-16	*Chandra*	969		not in FOV	
1999-12-27	*Chandra*	790		not in FOV	
2000-06-03	XMM-Newton	0125960101	39.2	$<4.3 \times 10^{-14}$	<0.03
2000-06-04	XMM-Newton	0125960201	14.2	$<1.8 \times 10^{-14}$	<0.01
2000-08-16	*Chandra*	383	2.16	$<8.8 \times 10^{-15}$	<0.007
2000-12-14	XMM-Newton	0110900101	29.6	6.3×10^{-13}	0.5
2003-06-19	XMM-Newton	0152020101	110.5	$<3.6 \times 10^{-15}$	<0.003
2003-09-19	*Chandra*	3931	83.6	$<4.4 \times 10^{-15}$	<0.003

[a] 0.3−10 keV luminosity assuming a distance of 2.58 Mpc and a bremsstrahlung model (kT = 2.24 keV, $N_H = 1.74 \times 10^{20}$ cm^{-2}).

We applied the source detection tasks `eboxdetect` and `emldetect` only on the data from the PN detector, as the source was positioned far from the optical axis and close to the edge of the FOV on the MOS detectors. The obtained position was then corrected using optical reference coordinates from the USNO B1 catalogue (Monet et al. 2003) of three AGN, identified by Vogler & Pietsch (1999, sources X4, X22, X58). The corrected position in J2000 coordinates is α = 00h48m20.11s, $\delta = -25°10'10\farcs4$ with an error in position of $0\farcs3$. The derived position is well within the positional errors given by LB2005 for NGC 253 ULX1.

A foreground star with a B magnitude of ∼13 (Monet et al. 2003) is located close (15.5″) to the obtained position (Fig. 3). We can rule out that the actual detection of NGC 253 ULX1 in observation 0110900101 was caused by this star, as its proper motion of −9.2 mas/yr in RA· cos(Dec) and −3.6 mas/yr in Dec (Zacharias et al. 2004) is too small to match the detected position of NGC 253 ULX1 with that of the star within the period of observations. Additionally there was no detection of the source in other XMM-Newton observations using the same filter.

We extracted energy spectra for NGC 253 ULX1 for all EPIC detectors. For the PN chip we included source counts from an elliptical region with major and minor axes of 27.6″ and 12.3″ respectively. The background region was a circular source-free region with a radius of 48″ on the same CCD close to the source. For MOS the source extraction region was an ellipse with major (minor) axes of 28.95″ (11.3″) for MOS1 and 31.35″ (15.15″) for MOS2, respectively. The background regions were circles with radii of 68″ and 80″ for MOS1 and MOS2, respectively. After subtracting the background the spectra for each instrument were rebinned to a significance level of 3σ.

For the spectral analysis XSPEC 11.3.1 was used. The best-fit parameters from different models provided within XSPEC are listed in Table 2. Using the PN and MOS spectra simultaneously the source spectrum was best fitted with a bremsstrahlung model (Fig. 1). The fit of the multicolour disk blackbody model (diskpn) would also be acceptable. However, we favour the bremsstrahlung model since it is less complex and gives a better χ^2_{red}. Except for the bremsstrahlung model the foreground absorption (N_H) had to be fixed to the Galactic foreground absorption as a lower limit (1.30×10^{20} cm^{-2}, Dickey & Lockman 1990). If the parameter was free to adjust it converged to unreasonably low values.

Table 2. Models for the source spectrum of NGC 253 ULX1.

Model[a]	N_H[b] (10^{20} cm^{-2})	Model parameter	χ^2_{red}
po	1.30	$\Gamma = 1.94 \pm 0.05$	1.663
bremss	$1.74^{+0.02}_{-0.01}$	$kT = 2.24^{+0.38}_{-0.31}$ keV	0.961
mekal	1.30	$kT = 3.17 \pm 0.19$ keV	2.042
diskbb	1.30	$kT = 0.62 \pm 0.04$ keV	1.671
diskpn	1.30	$kT = 0.69^{+0.06}_{-0.07}$ keV	1.366
		$R = 5.34^{+9.79}_{-2.34}\, R_S$	

[a] po: power law; bremss: thermal bremsstrahlung; mekal: Mekal thermal plasma; diskbb: multiple blackbody disk; diskpn: accretion disk around a black hole.
[b] All models are modified by foreground absorption (XSPEC model `wabs`).

From the best fitting spectral model we calculated the source flux and, assuming a distance of 2.58 Mpc (Puche et al. 1991) we derived an unabsorbed luminosity of 5.0 × 10^{38} erg s^{-1} in the 0.3−10.0 keV band.

In order to study the temporal behaviour of the source a background corrected light curve was created using the tasks `evselect` and `lccorr`. The source count rate was constant at about 0.8 ct s^{-1} within the errors of about 15% during observation 0110900101.

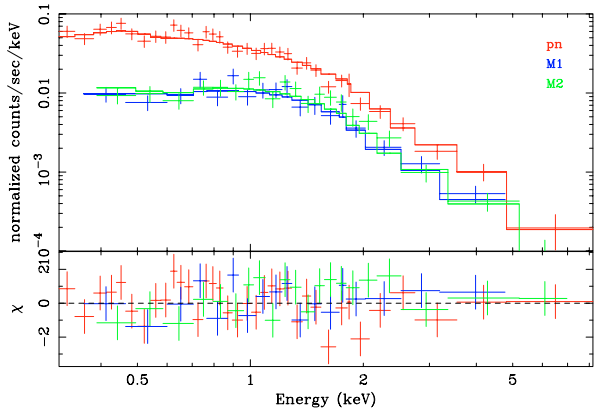

Fig. 1. Comparison of the PN and MOS spectra of NGC 253 ULX1 with the best-fit bremsstrahlung model. In the lower panel the residuals (in units of σ) between data and model are shown.

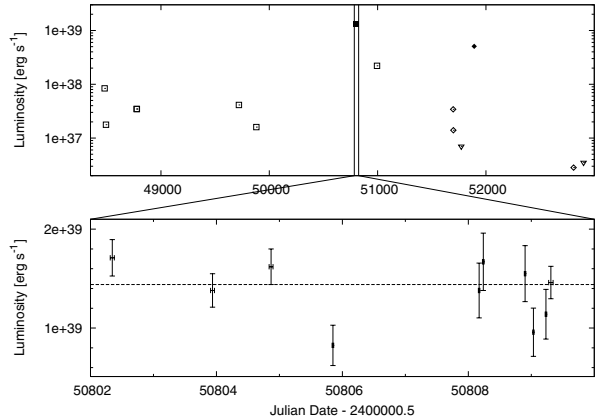

Fig. 2. Light curve of NGC 253 ULX1. *Upper panel*: solid symbols represent detections, open symbols 3σ upper limits of NGC 253 ULX1. Different instruments are represented by different symbols: *ROSAT* (squares), XMM-Newton (diamonds) and *Chandra* (triangles). *Lower panel*: single *ROSAT* HRI exposures with errorbars from observation 601111h where the source was detected. The length of each observation is indicated by the x-errorbar. In contrast to the upper panel the lower panel plot is linear in luminosity.

4. Analysis of ROSAT observation 601111h

The first detection of NGC 253 ULX1 was in *ROSAT* observation 601111h (LB2005). The observation (total exposure time 17.5 ks) is spread over ten observing intervals, with different exposure and waiting time for the individual observations. The source was bright enough to determine luminosities for each of these observation intervals.

We calculated count rates using the EXSAS source detection task `detect/sources`. To reduce noise we only analysed HRI channel 2−15. We used WebPIMMS (v3.6c) and the spectral model retrieved from the XMM-Newton observation (bremsstrahlung, $kT = 2.24$ keV, $N_{\rm H} = 1.74 \times 10^{20}$ cm^{-2}) to determine energy conversion factors to obtain the corresponding fluxes and luminosities (see lower panel of Fig. 2). The luminosity averaged over the whole observation (1.43×10^{39} erg s^{-1}) is indicated by the dashed line.

During the observation the source showed significant variability by at least a factor of 2.

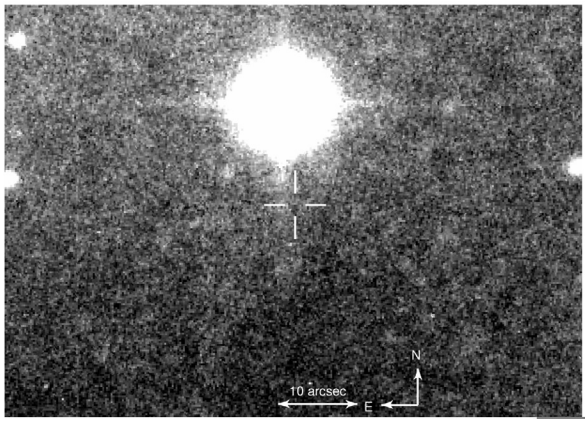

Fig. 3. *R*-band optical image taken with the Wide Field Imager on the MPG-ESO 2.2 m Telescope. The source is located close to a ∼13 mag star. The *R* magnitude is 24.2.

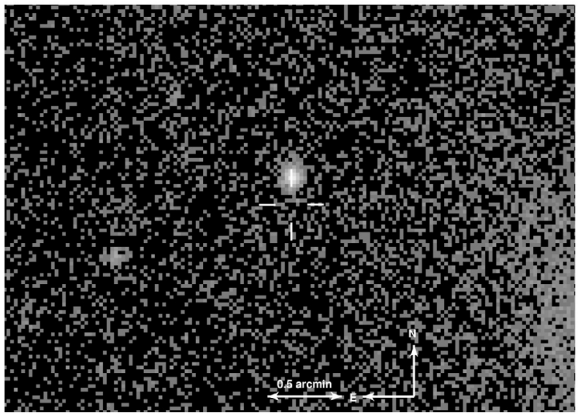

Fig. 4. Near UV image taken with GALEX. The NUV magnitude is 22.

5. Discussion

We detected the recurrence of NGC 253 ULX1 in the XMM-Newton observation from 2000 December 14. This was the first detection after the outburst in 1997, reported from *ROSAT* HRI observations by LB2005. In all other observations of NGC 253 the luminosity of the source was below the detection limit. This implies brightness variability by at least a factor of 500. Its fastest change in luminosity ($L_{\rm max}/L_{\rm min}$) exceeds a factor of 71 in 120 days.

The improved position (errors of $0\farcs24$ compared to $4''-10''$) of the source determined in Sect. 3 allowed us to search for optical counterparts. We checked images taken with the Wide Field Imager (WFI) on the MPG-ESO 2.2 m Telescope at La Silla in the *R*- (Fig. 3), *I*- and *B*-band (limiting magnitudes 24.2, 22.9 and 24.3, respectively) and images taken with the Galaxy Evolution Explorer (GALEX, a space telescope from NASA observing in the ultraviolet) in the NUV (Fig. 4) and FUV (limiting magnitudes 22 and 23, respectively), but no counterpart could be detected.

With the data discussed in Sects. 3 and 4 we can exclude that NGC 253 ULX1 is either a foreground object or a background AGN based on three arguments: (i) We estimated the $\log(f_{\rm X}/f_{\rm opt}) = \log f_{\rm X} + (m_{\rm V}/2.5) + 5.37 > 3.2$ using the flux of the *ROSAT* detection and a lower limit for $m_{\rm V}$ of 24.2

(averaging the limiting magnitudes of the *R*- and the *B*-WFI images, see above). Following Maccacaro et al. (1988) this value exceeds that expected for galactic sources (−4.6 to −0.6) as well as AGNs (−1.2 to +1.2); (ii) the variability of NGC 253 ULX1 is by a large factor higher than the typical value observed for AGNs (∼10−60); (iii) NGC 253 ULX1 shows a bremsstrahlung spectrum, whereas spectra of AGNs above 2 keV are typically fitted by a power law. The recurrent outbursts also exclude that the source is the luminous remnant of a recent supernova, like e.g. SN1993J in M 81 (Zimmermann & Aschenbach 2003).

The X-ray spectrum may indicate that NGC 253 ULX1 is a low mass X-ray binary (LMXB). The X-ray emission in these objects is created in the optically thin boundary layer between the disk and the neutron star and comptonization may dominate the spectral emission (White et al. 1988), leading to a spectrum that can be fitted with a bremsstrahlung model. However the *ROSAT* HRI peak luminosity of 1.43×10^{39} erg s^{-1} is very high for typical LMXBs. Other systems that show bremsstrahlung spectra are black hole XRBs, e.g. Cyg X-1 (Sunyaev & Truemper 1979), LMC X-3 and X1755-33 (White et al. 1988). These systems may contain a high or low mass companion.

An additional argument for a low mass companion comes from the lack of an optical counterpart (see above). High mass X-ray binaries (HMXBs) should be detectable at about 22 to 24 mag, extrapolating *V* magnitudes from HMXBs in the Magellanic Clouds (Liu et al. 2000). We would have detected an object of this brightness in the WFI data.

The luminosity of a compact object radiating at the Eddington limit is given as $L_{\rm Edd} = 1.5 \times 10^{38}\,(M/M_\odot)$ erg s^{-1}, when electron scattering dominates the opacity. Luminosities higher than 2×10^{38} erg s^{-1} (corresponding to a 1.4 $M_\odot$ object, commonly assumed as the maximum mass of a neutron star) suggests that the compact object is a black hole. According to NGC 253 ULX1's maximum luminosity of 1.43×10^{39} erg s^{-1} the lower limit for the mass of the black hole is 11 $M_\odot$. Therefore NGC 253 ULX1 is not required to be an IMBH.

Another argument against an IMBH is the temperature of NGC 253 ULX1. Miller et al. (2004a) compared intermediate mass black hole candidate ULXs and stellar mass black holes with respect to luminosity and temperature. If we assume the multicolour disk blackbody model then NGC 253 ULX1's position in the luminosity-disk temperature diagram (Fig. 2 in Miller et al. 2004a) indicates that NGC 253 ULX1 is not an IMBH, but a stellar mass black hole.

Recently another object was found that, like NGC 253 ULX1, showed also a bremsstrahlung spectrum: X-44 in the Antennae Galaxies (NGC 4038/4039) (Miller et al. 2004b). The temperature of X-44 is 3.7 ± 0.5 keV and its luminosity is $1.0^{+1.3}_{-0.2} \times 10^{40}$ erg s^{-1}. This temperature is about a factor of 1.5 higher than in NGC 253 ULX1, and the luminosity exceeds the luminosity of NGC 253 ULX1 by a factor of 15 compared to the outburst in 1997.

Another interesting ULX to compare NGC 253 ULX1 with is M 101 ULX-1 (Kong et al. 2005). It was the first ULX that like NGC 253 ULX1 has been observed during more than one ultra-luminous outburst. Like many other ULXs the spectrum of M 101 ULX-1 is best described with an absorbed blackbody model, but the temperature of ∼50−160 eV is rather low. M 101 ULX-1 has a peak luminosity of about 10^{41} erg s^{-1} (0.3−7 keV), and the hardness of its spectrum changed between different observations. We do not know whether the spectrum of NGC 253 ULX1 changed in the two observations, as the XMM-Newton data provided the very first spectrum of the source. During 12 years of observations NGC 253 ULX1 showed two outbursts with an interval of three years. In M 101 ULX-1 the two outbursts are only seperated by half a year. On shorter time scales NGC 253 ULX1 showed only one drop in luminosity by a factor of ∼2 during the *ROSAT* observation, and in the XMM-Newton observation (exposure time 8.2 h) no variability could be detected. M 101 ULX-1 on the other hand does show short-time-scale variability. Its luminosity changed by a factor of $\gtrsim$10 on a time scale of hours. The lack of short time variability of NGC 253 ULX1 argues against the relativistic beaming model, since this would require a very stable jet (Reynolds et al. 1997).

Acknowledgements. We thank G. Szokoly for providing us with the images of NGC 253 from the Wide Field Imager, which are based on observations made with ESO Telescopes at the La Silla and Paranal Observatory. Some of the data presented in this paper were obtained from the Multimission Archive at the Space Telescope Science Institute (MAST). STScI is operated by the Association of Universities for Research in Astronomy, Inc., under NASA contract NAS5-26555. Support for MAST for non-HST data is provided by the NASA Office of Space Science via grant NAG5-7584 and by other grants and contracts. The XMM-Newton and the *ROSAT* project is supported by the Bundesministerium für Bildung und Forschung/Deutsches Zentrum für Luft- und Raumfahrt (BMBF/DLR), the Max-Planck Society and the Heidenhain-Stiftung. M.B. acknowledges support from the International Max Planck Research School on Astrophysics (IMPRS).

References

Begelman, M. C. 2002, ApJ, 568, L97
Dickey, J. M., & Lockman, F. J. 1990, ARA&A, 28, 215
King, A. R., Davies, M. B., Ward, M. J., Fabbiano, G., & Elvis, M. 2001, ApJ, 552, L109
Kong, A. K. H., Rupen, M. P., Sjouwerman, L. O., & Di Stefano, R. 2005, [arXiv:astro-ph/0503465]
Liu, J., & Bregman, J. N. 2005, ApJS, 157, 59
Liu, Q. Z., van Paradijs, J., & van den Heuvel, E. P. J. 2000, A&AS, 147, 25
Maccacaro, T., Gioia, I. M., Wolter, A., Zamorani, G., & Stocke, J. T. 1988, ApJ, 326, 680
Makishima, K., Kubota, A., Mizuno, T., et al. 2000, ApJ, 535, 632
Miller, J. M., Fabian, A. C., & Miller, M. C. 2004a, ApJ, 614, L117
Miller, J. M., Zezas, A., Fabbiano, G., & Schweizer, F. 2004b, ApJ, 609, 728
Monet, D. G., Levine, S. E., Canzian, B., et al. 2003, AJ, 125, 984
Puche, D., Carignan, C., & van Gorkom, J. H. 1991, AJ, 101, 456
Reynolds, C. S., Loan, A. J., Fabian, A. C., et al. 1997, MNRAS, 286, 349
Sunyaev, R. A., & Truemper, J. 1979, Nature, 279, 506
Vogler, A., & Pietsch, W. 1999, A&A, 342, 101
White, N. E., Stella, L., & Parmar, A. N. 1988, ApJ, 324, 363
Zacharias, N., Urban, S. E., Zacharias, M. I., et al. 2004, AJ, 127, 3043
Zimmermann, H.-U., & Aschenbach, B. 2003, A&A, 406, 969